Intelligent Automation And Soft Computing, 2018

Vol.24,no.3581–592

The Virtual Prototype Model Simulation on the Steady-state Machine Performance

Huanyu Zhao, Guoqiang Wang, Shuai Wang, Ruipeng Yang, He Tian, Qiushi Bi

College of Mechanical Science and Engineering, Jilin University, Changchun, P.R. China

ABSTRACT

Articulated tracked vehicles have high mobility and steering performance. The unique structure of articulated tracked vehicles can avoid the subsidence of tracks caused by high traction from instantaneous braking and steering. In order to improve the accuracy of the steady-state steering of the articulated tracked vehicle, the velocity of both sides of the track and the deflection angle of the articulated point need to match better to achieve the purpose of steering accurately and reduce energy consumption and wear of components. In this study, a virtual prototype model of the articulated tracked vehicle is established based on the multi-body dynamic software RecurDyn. The trend of the driving torque and power of each track changes as the velocity difference of two sides of the tracks and the traveling trajectory of the mass center of the front vehicle change in a specific condition are obtained by the experiment. The experimental results are compared and verified with the results obtained from the virtual prototype simulation. The change law of driving power in the steady-state steering process on the horizontal firm ground as changing the velocity difference of two sides of the tracks, the theoretical steering radius, and the ground friction is obtained by the virtual prototype model simulation analysis. The steering inaccuracy and track slip rate are used as indexes in evaluating the steady-state steering performance of the articulated tracked vehicle. The research provides references for the study of steady-state steering performance of articulated tracked vehicles.

KEY WORDS: Articulated tracked vehicles, Steady-state steering performance, Virtual prototype model simulation, Steering inaccuracy, Slip rate

1 INTRODUCTION

ARTICULATED tracked vehicles have the advantages of high mobility and good steering performance (Fijalkowski, 2003), which contribute to widespread use in the military, agriculture, forestry, and other fields. The unique structure of articulated tracked vehicles can avoid the subsidence of tracks caused by high traction from instantaneous braking and steering (Nuttall, 1964). In addition, the risk of rollover in the running process, as heavy wheeled vehicles (Edgar et al., 2011), is avoided. The steering of articulated tracked vehicles differs from that of four-tracked (Watanabe et al., 1995) or multi-tracked vehicles (Zongwei et al., 2013) because the articulated component is comprised of two sets of crawlers in a series together. Articulated tracked vehicles have two main forms. The first form is a wagon-type articulation of tracked vehicles, such as towing vehicles, that enables a tracked trailer to drive through a drawbar (Alhimdani, 1982; Basher, 2012). The other is composed of two powerful vehicles that use the moment applied on the articulated component between the two sets of crawlers to make each crawler deflect from the other to achieve steering. Articulated crawlers have a certain inaccuracy in the steady-state steering, namely, understeer and oversteer. Inaccurate steering can cause the crawler to excessively slip or skip in the steering process, resulting in excessive wearing and reduced life of parts and increased energy loss. Therefore, conducting a study on the steady-state steering performance of an articulated crawler is necessary.

CONTACT Qiushi Bi biqiushijlu@163.com

Many scholars have conducted a study on articulated tracked vehicles. Sasaki et al. (Sasaki et al., 1991) described the articulated tracked vehicle design and its unique features and operating characteristics. They also presented the experimental data of the articulated tracked vehicle that drives on different angles and slopes through hydraulic control. On the basis of single-tracked vehicles (Kitano & Jyozaki, 1976; Kitano & Kuma, 1977) and the steering performance of coupled-tracked vehicles (non-articulated) (Kitano et al., 1981) in the steady and unsteady-state transition process, Watanabe et al. (Watanabe & Kitano, 1986) constructed a mathematical model of the unsteady process of articulated crawler vehicles on horizontal ground and performed an experimental demonstration with a proportional model. They concluded that articulated tracked vehicles require lesser driving torque and track slip rate than single-tracked and non-articulated double-tracked vehicles.

Establishing a theoretical model about the running process of articulated crawlers is complex. The interaction between the track shoe and the firm ground (Wong, & Chiang, 2001) or the soft ground (Wong, 2009; Al-Milli, 2010) is also complex. With the continuous development of virtual prototyping technology, the virtual prototype model is widely used to perform a simulation analysis of the driving performance of tracked vehicles (Janarthanan et al., 2012; Choi et al., 1998; Lee et al., 1998; Wang et al., 2014). Wong (Wong, 1992; Wong, 1992) analyzed the influence of important parameters, such as joint articulation configuration, suspension characteristics, initial track tension, track width, and center of gravity location, on the mobility of tracked vehicles by using the computer simulation model. The experiment showed that the simulation model plays an important role in the optimization design of tracked vehicles. The efficiency of the simulation analysis of the steady-state steering performance of an articulated crawler will be greatly improved by constructing an accurate articulated crawler virtual prototype model.

It can be seen from the above research, the articulated tracked vehicle was not driven by the motor alone on each track and only an articulated device was used to deflect the articulated crawler. For a motor-operated articulated crawler, the velocity difference of two sides of the tracks, the theoretical steering radius, and the ground friction coefficient can all have a considerable impact on the steering performance of the articulated crawler. In this study, each track of the articulated crawler is driven by a motor. The influence of three important factors on the steering performance of articulated tracked vehicle is analyzed.

In this paper, the accuracy of the virtual prototype model is experimentally validated through an experimental prototype. The accurate virtual prototype model is utilized to perform a simulation analysis on the driving power of the crawler and the trajectory change of the front vehicle when the articulated tracked vehicle is moving in steady-state on the horizontal firm ground. The simulation included changing the velocity difference, the theoretical steering radius, and the ground friction coefficient. The simulation results provide a reference for the study on the steering control of articulated tracked vehicles.

2 ESTABLISHMENT OF VIRTUAL PROTOTYPE MODEL

FIGURE 1 shows the virtual prototype model of an articulated crawler established in the low-speed module Track_LM of multi-body dynamic software RecurDyn. The main parameters of the model are shown in Table 1. Rear vehicles are indicated by “”. The maximum velocity of the designed articulated crawler is 0.2 m/s. In the virtual prototype model, the front and rear vehicles are connected by two articulated frames, which are operated by a linear actuator to deflect the front and rear vehicles around the articulated point.

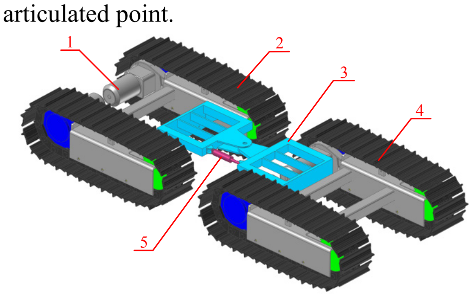

Figure 1. Virtual Prototype Model of the Articulated Crawler: 1 Drive motor, 2 Rear vehicle, 3 Articulated frame, 4 Front vehicle, and 5 Linear actuator.

Table 1. Main Parameters of the Articulated Crawler.

Parameters	Values
Mass: $G=G'$	450 kg
Ground contact length: $L=L'$	1200 mm
Ground contact pressure: $P=P'$	6.125 kPa
Track gauge: $B=B'$	930 mm
Width of link pad: $b=b'$	300 mm
Pitch of chain link: $p_c=p_c'$	102 mm
Pitch radius of sprocket: $r=r'$	152 mm
Tooth number of sprocket: $n_s=n_s'$	21
Distance from articulation point to mass center: $l=l'$	788 mm
Number of track rollers: $n=n'$	2
Number of chain links: $n_c=n_c'$	27
Deflection angle range	±20°

3 EXPERIMENTAL VERIFICATION

GIVEN that conducting a theoretical verification of the veracity of the virtual prototype is unpractical, verifying the accuracy of the virtual prototype model by experiment is necessary. Figure 2 illustrates the experimental prototype of the articulated crawler. The crawler is operated by motors with a rated power and speed of 0.75 kW and 1250 rpm respectively. The reduction ratio of the reducer is 100. The frequency converters are used to change frequency between the power supply and motors. The motor speed is changed by controlling the output frequency of the frequency converters through the computer, and then the velocities of both sides of the crawler are controlled. The stabilized power supply is used to supply 24V DC voltage to the linear actuator. The articulated steering part relies on the push and pull of the linear actuator to adjust the steering angle and direction. A trajectory drawing device depicts the trajectory of the mass center of the front vehicle of the articulated crawler.

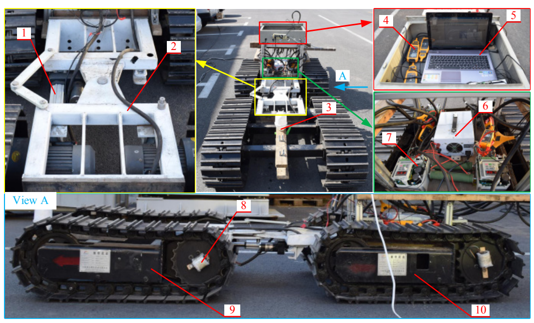

Figure 2. Experimental Prototype of the Articulated Vehicle: 1 Linear actuator, 2 Articulated frame, 3 Trajectory drawing device, 4 Frequency meter, 5 Laptop, 6 Stabilized power supply, 7 Frequency converter, 8 Torque sensor, 9 Front vehicle, and 10 Rear vehicle.

3.1 Comparison of trajectories

The articulated crawler runs on the firm ground at a velocity of 0.15 m/s for 30 s at the beginning. Then, the velocity of the left side (inside) of the articulated crawler decreases to 0.13 m/s, whereas the velocity of the right side (outside) of the articulated crawler increases to 0.17 m/s. Meanwhile, the linear actuator elongates at a speed of 5 mm/s to push the articulated point to turn 20°, thereby enabling the crawler to turn left until it runs steadily. Figures 3(a) and (b) show the comparison of the simulation and experimental trajectories of the mass center of the front vehicle of the articulated crawler. A certain lateral slip occurs in the running process of the crawler, causing the second path to be slightly outward compared to the first path in the simulation result. In the experimental results, the deviation of the two trajectory paths is not obvious because of the error of the trajectory drawing device. The deviation of the two paths is small, and the lines of the delineation are rough. However, the consistency of the comparison results is acceptable based from the results of the overall trajectory process.

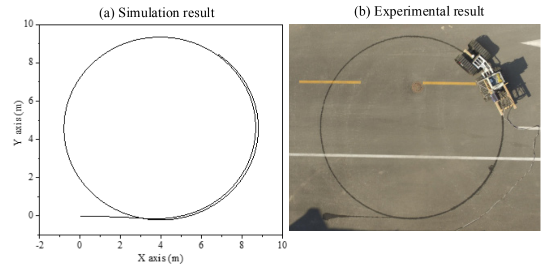

Figure 3. Trajectory Comparison of Simulation and Experiment.

3.2 Comparison of Driving Torque and Power of Simulation and Experimental Results

Figures 4 and 5 show the comparison of the simulation and experimental results of the average driving torque and the power of the articulated crawler in steady-state at 20° articulated point steering and velocity differences of two sides of the tracks at 0, 0.02, 0.04, and 0.06 m/s, respectively. In Figure 4, the driving torque of the same-side tracks is similar. The driving torque of the left and right side tracks decreases and increases, respectively, as the velocity difference increases. The change trend of the driving power of each track is similar to that of the driving torque, as shown in Figure 5. The simulation and experimental results in Figures 4 and 5 are similar, and the overall change trends are also similar; thus, the consistency is acceptable.

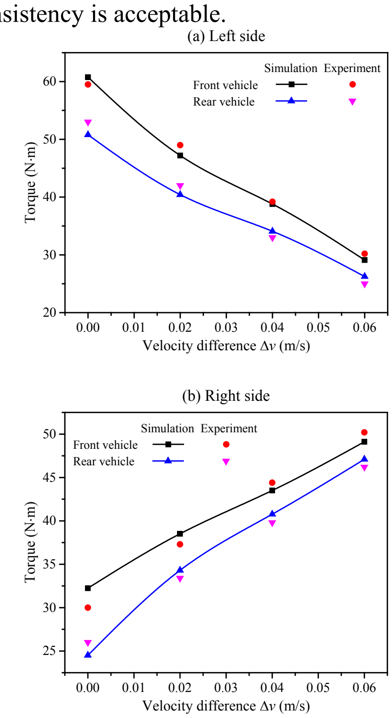

Figure 4. Average Torque Comparison of Simulation and Experiment.

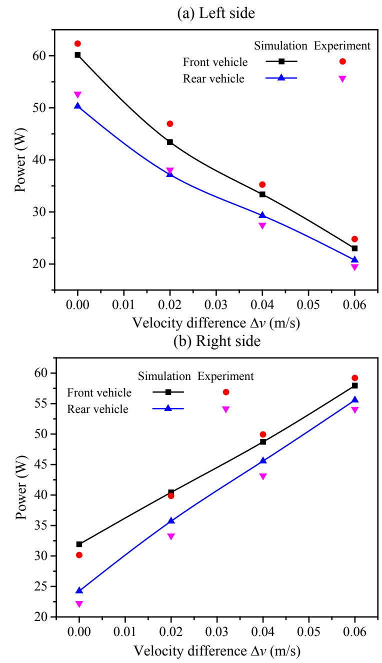

Figure 5. **Average Power Comparison of Simulation and Experiment.**

The virtual prototype model can describe the running performance of the articulated crawler. Therefore, the steering performance of the articulated crawler can be analyzed and studied.

4 RESULTS AND DISCUSSIONS

4.1 Steering Inaccuracy and Slip Rate

IN the steering process of the articulated crawler, each track is affected by the lateral force and existing slips or skips (Zongwei et al., 2013). Figure 6 shows the diagram of the steering motion of the articulated crawler. Each track has a respective velocity instantaneous center O_{si} (i=1, 2, 3, 4) on the ground plane, which is relative to the geometric center of the track–terrain interface O_i that produces longitudinal D_i and lateral offset A_i. O_L is the theoretical steering center and O_S is the actual steering center of the articulated tracked vehicle. The distance between O_S and O_L, and the mass center of the front vehicle or rear vehicle (C_1 or C_2) are the actual steering radius R_S and theoretical steering radius R_L respectively. The steering inaccuracy is expressed as

$$\delta_R = (R_S - R_L) / R_L \times 100\% \tag{1}$$

Where the theoretical steering radius R_L is expressed as

$$R_L = l / \tan(\alpha / 2) \tag{2}$$

Where α is the deflection angle of the articulated point. When R_S>R_L, δ_R>0, that is, understeer; when R_S<R_L, δ_R<0, that is, oversteer; when δ_R approaches 0, the steering trajectory is ideal. Therefore, the steering accuracy of the articulated crawler can be evaluated by the steering inaccuracy δ_R.

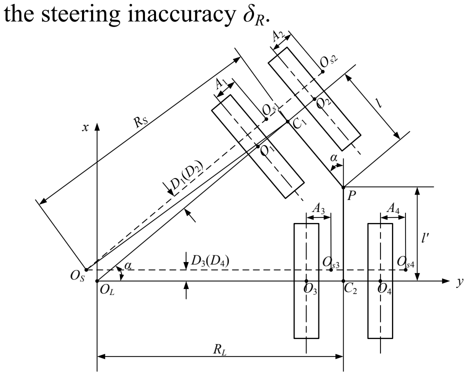

Figure 6. **Steering Motion Diagram.**

The skip occurs when the relative velocity (winding velocity) v_t of the track is greater than the entrainment velocity (translational velocity) v_e, and the slip occurs when the relative velocity v_t is less than the entrainment velocity v_e (Zongwei et al., 2013). Thus, the slip rate δ_S can be introduced to quantitatively describe the extent to which the track–terrain interface is skipping or slipping. It is defined as

$$\delta_S = (v_t - v_e) / v_t \times 100\% \tag{3}$$

When v_t>v_e, δ_S>0, skip occurs in the track; when v_t<v_e, δ_S<0, slip occurs in the track; when δ_S approaches 0, the running efficiency of track is the highest. Therefore, the running stability of the tracks can be evaluated by the slip rate δ_S.

4.2 Effect of Velocity Difference and Theoretical Steering Radius

To maintain the running velocity v_s, that is the velocity of the mass center of the articulated crawler, in the overall running process, in the case of going straight, the relationship between the inner v_1 and outer track velocities v_2 is v_1=v_2=v_s; whereas in the case of steering, the inner track velocity v_1 is decreased and the outside track velocity v_2 is increased to form a velocity difference Δv=v_2-v_1. The velocity of both sides of the tracks is shown in Table 2. The relationship between the deflection angle of the linear actuator pushing the articulated point and the theoretical steering radius is when α=20°, R_L=4.47 m; when α=15°, R_L=6.00 m; when α=10°, R_L=9.01 m; when α=5°, R_L=18.05 m. The ground friction coefficient is 0.7.

Table 2. **Velocity of Both Sides of the Articulated Crawler.**

	Velocity of center of mass: v_s (m/s)	Velocity of inside track: v_1 (m/s)	Velocity of outside track: v_2 (m/s)	Velocity difference: Δv (m/s)
1	0.15	0.15	0.15	0
2		0.14	0.16	0.02
3		0.13	0.17	0.04
4		0.12	0.18	0.06
5		0.11	0.19	0.08
6		0.1	0.2	0.1

Figure 7 shows the effect of velocity difference and theoretical steering radius on the driving power of each track. At the same Δv, the driving power of each track decreases with the increase of R_L. At the same R_L, the driving power of the left and right side tracks decreases and increases, respectively, with the increase of Δv. In addition, as the R_L increases, the driving power of both sides of the crawler slows down with the trend of Δv.

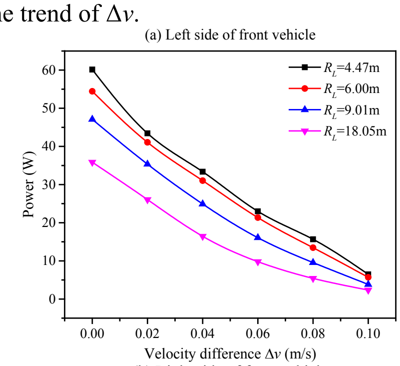

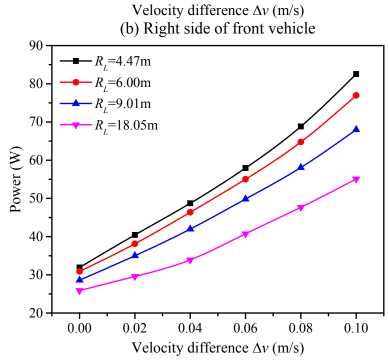

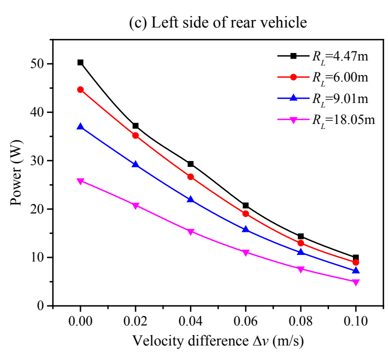

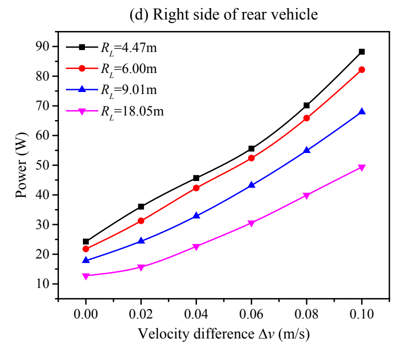

Figure 7. **Effect of Velocity Difference and Theoretical Steering Radius on Driving Power.**

Figure 8 shows the effect of the velocity difference and the theoretical steering radius on the total driving power of the articulated crawler. The change trend of the total driving power as the Δv increases at different R_L is the same, decreasing first and then increasing, and is relatively low at Δv of 0.02–0.06 m/s. In the same Δv change interval, the variation range of the total driving power increases as the R_L increases.

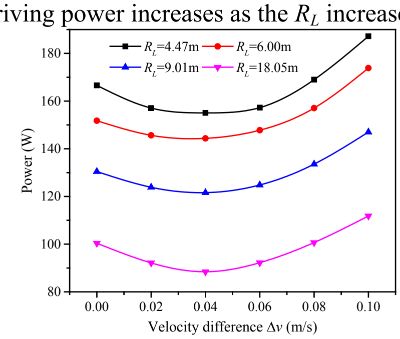

Figure 8. **Effect of Velocity Difference and Theoretical Steering Radius on Total Driving Power.**

Figure 9 shows the effect of the velocity difference on the trajectory of the mass center of the front vehicle under different theoretical steering radii. R_S decreases with the increase of Δv at the same R_L. In the same Δv change interval, the range of the mass center of the front vehicle R_S increases as the R_L increases.

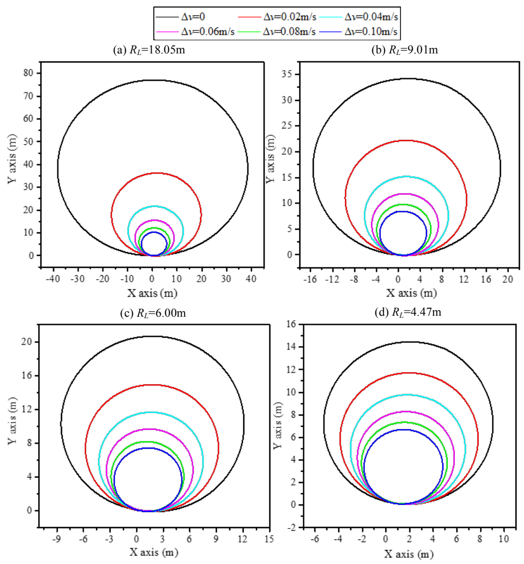

Figure 9. **Effect of Velocity Difference and Theoretical Steering Radius on Steering Trajectory.**

Figure 10 shows the variation of the steering inaccuracy of the articulated crawler with the velocity difference of two sides of the tracks under different theoretical steering radii. At the same R_L, the δ_R of the front vehicle becomes understeered to oversteered gradually with the increase of Δv, and the slope of δ_R curves decreases gradually. When Δv<0.04 m/s, the trend of δ_R curves changes faster with the increase of R_L. When Δv>0.04 m/s, the trend of δ_R curves is similar. When δ_R=0, the corresponding Δv decreases as the R_L increases. That is, if R_L=4.47 m, then Δv=0.05 m/s; if R_L=6.00 m, then Δv=0.04 m/s; if R_L=9.01 m, then Δv=0.03 m/s; if R_L=18.05 m, then Δv=0.02 m/s.

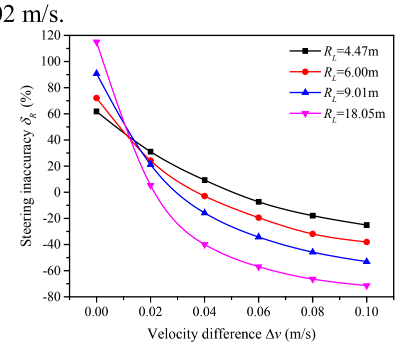

Figure 10. **Effect of Velocity Difference and Theoretical Steering Radius on Steering Inaccuracy.**

Figure 11 shows the variation of the slip rate of each track with the velocity difference under different theoretical steering radii. The change trend of δ_S of both sides of the articulated crawler is similar. At the same R_L, the tracks on the left side δ_S<0, that is, slip occurs; δ_S decreases with the increase of Δv; and the slope of δ_S curve gradually increases. Moreover, the tracks on the right side δ_S increases with an increase of Δv; from δ_S<0 it gradually increases to δ_S>0, that is, from slip to skip, and the slope of δ_S curve gradually decreases. At the same Δv, the δ_S of the left side tracks decreases with the increase of R_L. The δ_S of the right tracks increases with the increase of R_L.

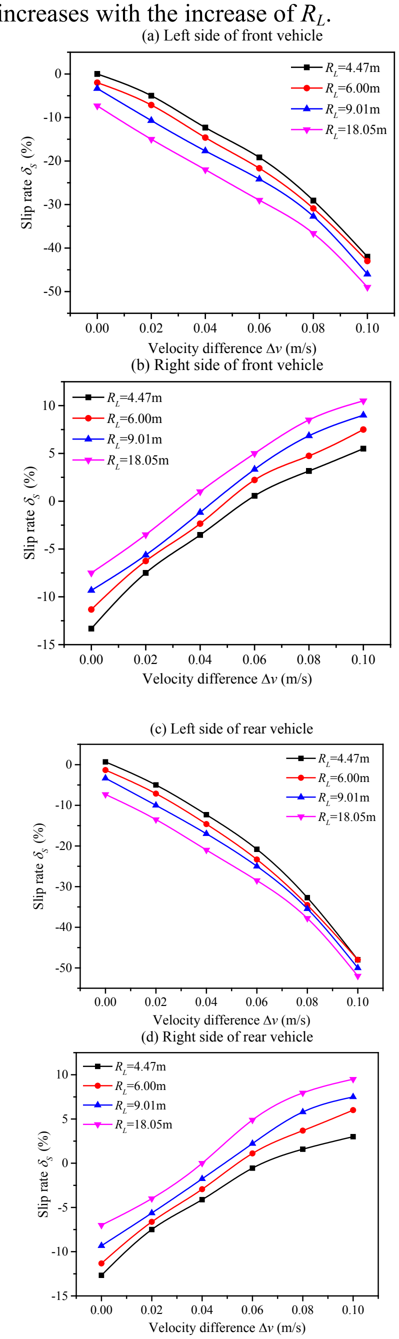

Figure 11. **Effect of Velocity Difference and Theoretical Steering Radius on Slip Rate.**

Figures 10 and 11 show that when δ_R=0, the corresponding velocity difference of the four theoretical steering radii is 0.05, 0.04, 0.03, and 0.02 m/s. The corresponding slip rate of the left track is approximately −15%, and the slip rate of the right track is approximately −2.5%. Thus, the slip rate is low. Figure 8 shows that each velocity difference is between 0.02 and 0.06 m/s, and the total driving power is low. Thus, the steady-state steering performance of the articulated crawler can be improved by the corresponding velocity difference of each theoretical steering radius.

4.3 Effect of Velocity Difference and Ground Friction Coefficient

In the case of the theoretical steering radius is 4.47 m, the effect of the ground friction coefficient and the velocity difference on the steady-state steering performance of the articulated crawler is analyzed. Figure 12 shows the effect of the velocity difference under different ground friction coefficients for each track driving power. At the same Δv, the driving power of each track increases as the ground friction coefficient μ increases. At the same μ, the driving power of the left and right side tracks decreases and increases, respectively, with the increase of Δv. In addition, as μ decreases, the trend of driving power for both sides of the tracks with Δv slowed down.

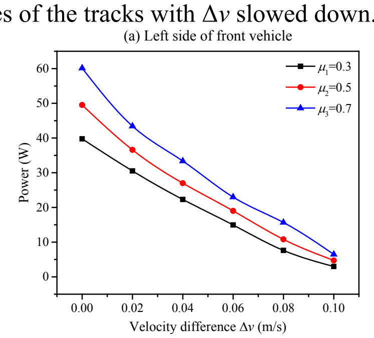

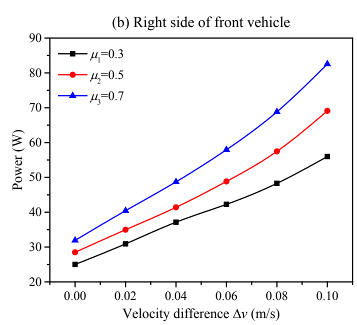

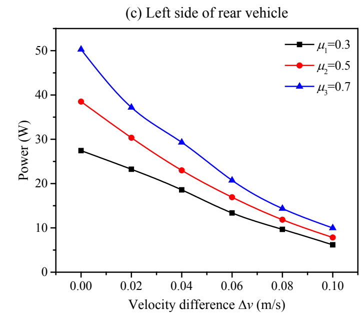

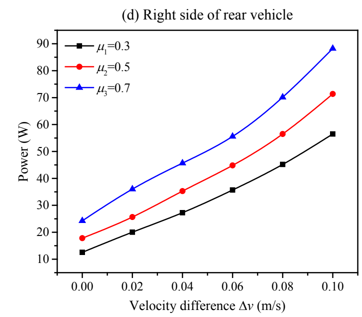

Figure 12. **Effect of Velocity Difference and Ground Friction Coefficient on Driving Power.**

Figure 13 shows the effect of velocity difference and ground friction coefficient on the total driving power of the articulated crawler. The trend of the total driving power of the articulated crawler changes as the Δv increases at different μ, which decreases first and then increases, and is relatively low at Δv of 0.02–0.06 m/s. In the same Δv change interval, the variation range of the total driving power increases as the μ increases.

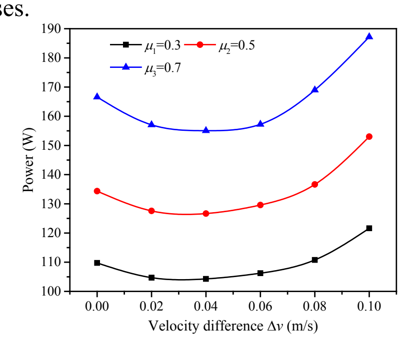

Figure 13. **Effect of Velocity Difference and Ground Friction Coefficient on Total Driving Power.**

Figure 14 shows the effect of the velocity difference on the trajectory of the mass center of the front vehicle under different ground friction coefficients. R_S decreases as the μ increases at the same Δv. In the same μ, the mass center of the front vehicle R_S decreases as the Δv increases.

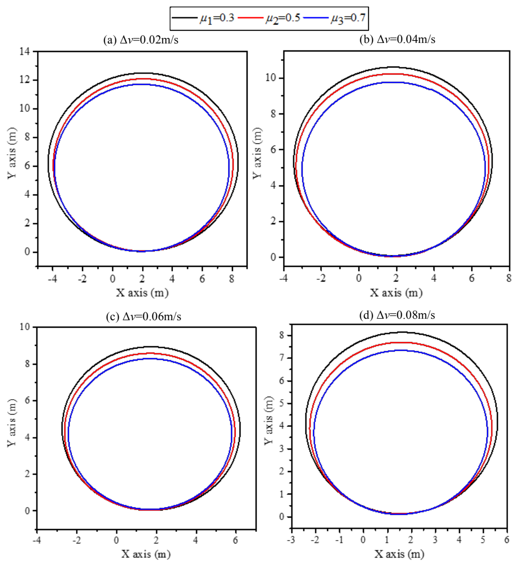

Figure 14. Effect of Velocity Difference and Ground Friction Coefficient on the Steering Trajectory.

Figure 15 shows the variation of the steering inaccuracy of the articulated crawler with the velocity difference under different ground friction coefficients. The change trend of the δ_R of the mass center of the front vehicle is the same as the Δv increases, and the δ_R of the front vehicle gradually becomes understeer to oversteer as the Δv increase. Moreover, the slope of δ_R curves gradually decreases. When δ_R=0, the corresponding Δv decreases as the μ increases. That is, if μ=0.3, then Δv=0.06 m/s; if μ=0.5, then Δv=0.055 m/s; if μ=0.7, then Δv=0.05m/s.

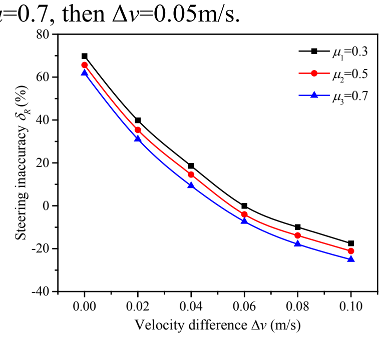

Figure 15. Effect of Velocity Difference and Ground Friction Coefficient on the Steering Inaccuracy.

Figure 16 shows the variation of the slip rate of each track with the velocity difference under different ground friction coefficients. The change trend for both sides of the tracks δ_S is similar. At the same μ, the tracks on the left side δ_S<0, that is, slip occurs, δ_S decreases as Δv increases, and the slope of δ_S curve gradually increases. Moreover, the tracks on the right side δ_S increases as Δv gradually increases from δ_S<0 to δ_S>0, that is, from slip to skip, the slope of δ_S curve gradually decreases. At the same Δv, the δ_S of the tracks in the left side increases as the μ increases. The δ_S of the tracks on the right side increases as the μ increases when the slip occurs, and δ_S decreases as the μ increases when the skip occurs. Therefore, the curve crosses when δ_S is approximately 0.

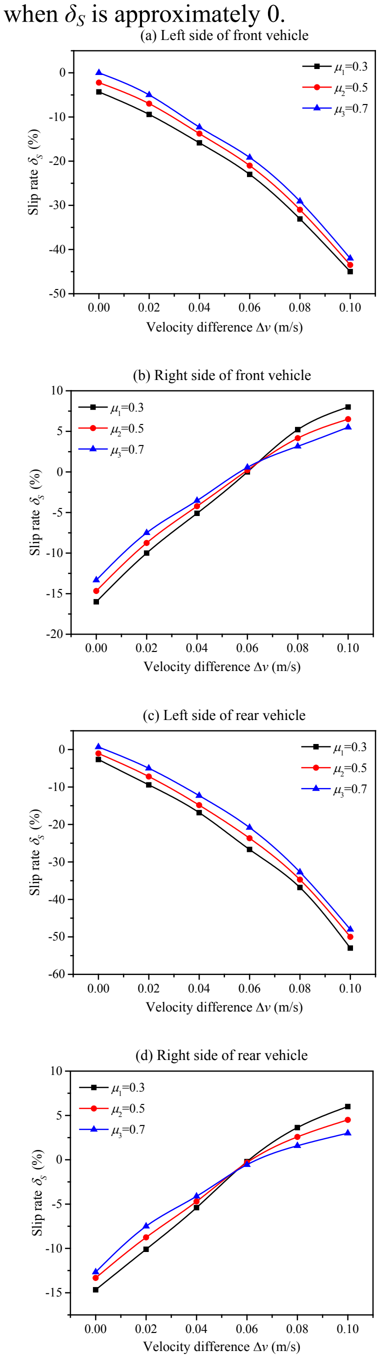

Figure 16. Effect of Velocity Difference and Ground Friction Coefficient on the Slip Rate.

Figures 15 and 16 show that when δ_R=0, the corresponding velocity difference of the three μ is 0.06, 0.055, and 0.05 m/s. In addition, the corresponding slip rate of the tracks on the left side is between −15% and −25%, and on the right side is between 0 and −2.5%. Figure 13 shows that the velocity difference is between 0.02 and 0.06 m/s, and the total driving power is low. Thus the steady-state steering performance of the articulated crawler can be improved by the corresponding velocity difference of each ground friction coefficient.

4.4 Comprehensive Effect of Velocity Difference, Theoretical Steering Radius, and Ground Friction Coefficient on Steering Performance

The effect of velocity difference, theoretical steering radius, and ground friction coefficient on the steady-state steering performance of the articulated crawler is comprehensively analyzed. Figures 17 (a) and (b) show the effect of velocity difference and ground friction coefficient on the steady-state steering inaccuracy of the articulated crawler in the case of theoretical steering radius of 18.05 and 9.01 m respectively. Figures 15 and 17 show that high R_L and μ results in the low Δv, which is required for stabilizing the articulated crawler δ_R at 0. For relative μ, R_L has a great effect on δ_R under the same Δv.

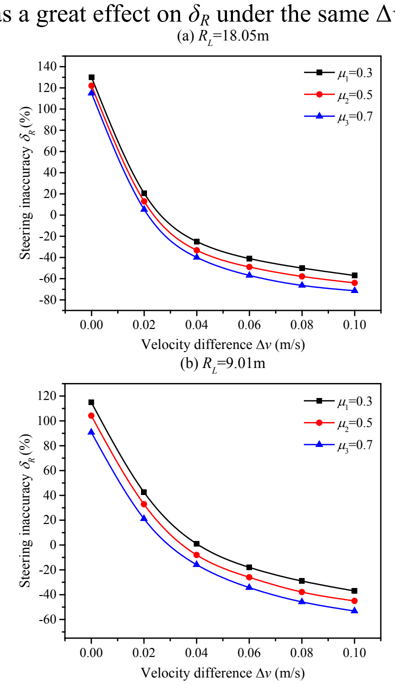

Figure 17. Effect of the Theoretical Steering Radius and Ground Friction Coefficient under Different Velocity Difference on Steering Inaccuracy.

Figures 18 and 19 show the effects of velocity difference and ground friction coefficient on each track slip rate in the case of theoretical steering radius of 18.05 and 9.01 m respectively. Figures 16, 18, and 19 show that as R_L and μ changes, the tracks on the left side slip under the same Δv, that is, δ_R<0. A high R_L and a low μ result in the decreased slip rate of the tracks on the left side under the same Δv. When the tracks on the right side slip, that is δ_R<0, the δ_R increases as the R_L and μ increase under the same Δv. When the tracks on the right side skip, that is δ_R>0, the δ_R increases as the R_L and μ decreases under the same Δv.

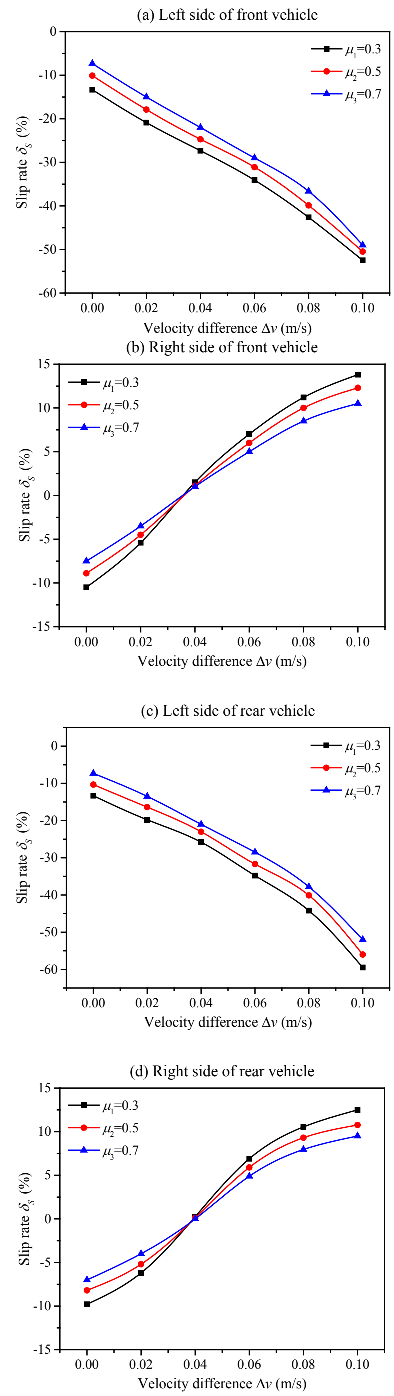

Figure 18. Effect of Ground Friction Coefficient and Velocity Difference under R_L =18.05 m.

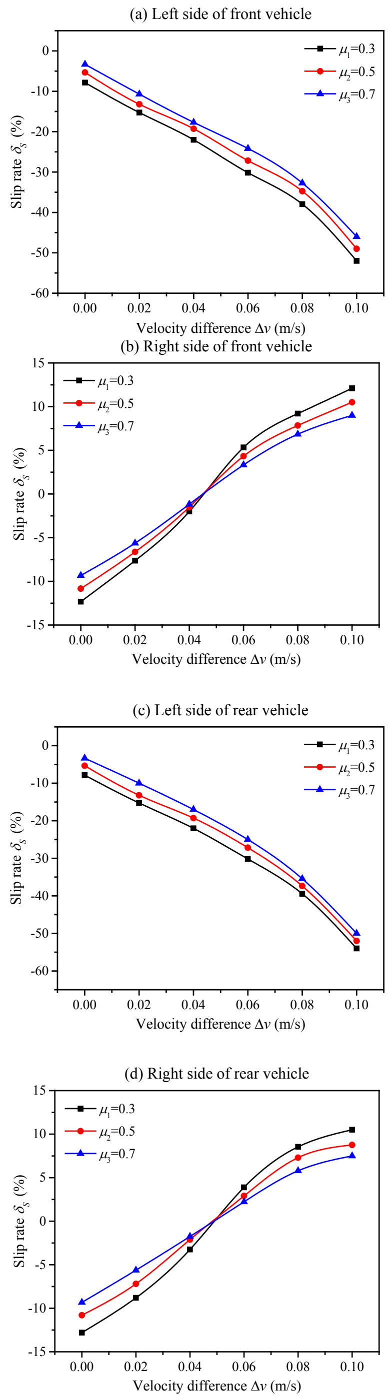

Figure 19. Effect of Ground Friction Coefficient and Velocity Difference under R_L=9.01 m.

Figures 17, 18, and 19 show that when δ_R=0, the velocity differences corresponding to the three μ when R_L=18.05 m are 0.03, 0.025, and 0.02 m/s; and the velocity differences corresponding to the three μ when R_L=9.01 m are 0.04, 0.035, and 0.03 m/s. The corresponding slip rate of the tracks on the left side is between −15% and −25%, the slip rate of track on the right side is between 0 and −2.5%.

5 CONCLUSIONS

ON the basis of the proposed virtual prototype simulation of RecurDyn and experimental verification methods, this research studied the impact of velocity difference, theoretical steering radius, and ground friction coefficient on the driving power of the articulated crawler, as well as the change of the trajectory of the front vehicle when the crawler moves in a steady-state on the horizontal firm road surface. The steady-state steering performance of an articulated crawler was likewise evaluated under different circumstances through the steering inaccuracy and the slip rate of each track.

Steering inaccuracy is used to evaluate the deviation between the actual and theoretical steering radii when the articulated crawler is in steady-state steering. When the theoretical steering radius and ground friction coefficient are high, the velocity difference which is required for stabilizing the steering inaccuracy at zero is low. The theoretical steering radius has a great effect on the steering inaccuracy under the same velocity difference.

The slip rate of the crawler is used to evaluate the slip or skip of the track during the steady-state steering of the articulated crawler. For the inside track, the slip usually occurs when changing the velocity difference, the theoretical steering radius, and the ground friction coefficient. For the outside track, both slip or skip may occur as the change of the velocity difference, the theoretical steering radius, and the ground friction coefficient. Under the corresponding velocity difference which improves the steering accuracy and reduces the driving power, the slip rate of both sides of the tracks is in a certain range.

When the theoretical steering radii and ground friction coefficients are different, the steering trajectory of the articulated crawler vehicle in the steady-state steering can be controlled effectively by selecting the appropriate velocity difference and conducting real-time monitoring of the crawler slip rate. Moreover, it can improve steering accuracy, reduce energy consumption, and improve operational efficiency. The research on the steady-state steering performance of articulated crawlers can be a reference for the study on steering control and trajectory optimization of articulated tracked vehicles.

6 ACKNOWLEDGMENTS

THIS work was supported by the Collaborative Innovation Center of Major Machine Manufacturing in Liaoning and Shanxi Provincial Key Scientific and Technological Projects (MJ2014-02).

7 REFERENCES

Alhimdani F. F., (1982). Steering analysis of articulated tracked vehicles. Journal of Terramechanics. 19(3), 195-209.

Al-Milli S., Seneviratne L. D. & Althoefer K. (2010). Track–terrain modelling and traversability prediction for tracked vehicles on soft terrain. Journal of Terramechanics. 47(3), 151-160.

Basher E. A., (2012). The Influence of Double Acting Hydraulic Piston on Tractive Forces for Towing Vehicle on Steering of Wagon Type Articulated Tracked Vehicle. Al-Rafadain Engineering Journal.

Choi J. H., Lee H. C. & Shababa A. A., (1998). Spatial Dynamics of Multibody Tracked Vehicles Part I: Spatial Equations of Motion. Vehicle System Dynamics. 29(1), 27-49.

Edgar N. S., Luis J. R., Reza L. & Danial S., (2011). Rollover prediction and control in heavy vehicles via recurrent high order neural networks. Intelligent Automation and Soft Computing. 17(1), 95-107.

Fijalkowski B. T., (2003). Novel mobility and steerability enhancing concept of all-electric intelligent articulated tracked vehicles. IEEE Transactions on Intelligent Transportation Systems. 225-230.

Janarthanan B., Padmanabhan C. & Sujatha C., (2012). Longitudinal dynamics of a tracked vehicle: Simulation and experiment. Journal of Terramechanics. 49(2), 63-72.

Kitano M. & Jyozaki H., (1976). A theoretical analysis of steerability of tracked vehicles. Journal of Terramechanics. 13(4), 241-258.

Kitano M. & Kuma M., (1977). An analysis of horizontal plane motion of tracked vehicles. Journal of Terramechanics. 14(4), 211-225.

Kitano M., Watanabe K., Sawagashira K. & Kinou. A., (1981). An analysis of plane motion of articulated tracked vehicles. Proceedings of ISTVS 7th International Conference. 111, 1413-1447.

Lee H. C., Choi J. H. & Shabana A. A. (1998). Spatial Dynamics of Multibody Tracked Vehicles Part II: Contact Forces and Simulation Results. Vehicle System Dynamics. 29(2), 113-137.

Nuttall C. J., (1964). Some notes on the steering of tracked vehicles by articulation. Journal of Terramechanics. 1(1), 38-74.

Sasaki S., Yamada T. & Miyata E., (1991). Articulated tracked vehicle with four degrees of freedom. Journal of Terramechanics. 28(2–3), 189-199.

Wang A., Gu Z. & Sun X., (2014). Dynamic simulation of acceleration for a foursprocket electric tracked vehicle under different pavement conditions. Transportation Electrification Asia-Pacific. IEEE.

Watanabe K. & Kitano M., (1986). Study on steerability of articulated tracked vehicles — Part 1. Theoretical and experimental analysis. Journal of Terramechanics. 23(2), 69-83.

Watanabe K., Kitano M. & Fugishima A., (1995). Handling and stability performance of four-track steering vehicles. Journal of Terramechanics. 32(6), 285-302.

Wong J. Y. & Chiang C. F., (2001). A general theory for skid steering of tracked vehicles on firm ground. Proceedings of the Institution of Mechanical Engineers Part D Journal of Automobile Engineering. 215(3), 343-355.

Wong, J. Y., (1992). Computer-aided methods for the optimization of the mobility of single-unit and two-unit articulated tracked vehicles. Journal of Terramechanics. 29(4-5), 395-421.

Wong J. Y., (1992). Optimization of the Tractive Performance of Articulated Tracked Vehicles Using an Advanced Computer Simulation Model. Proceedings of the Institution of Mechanical Engineers Part D Journal of Automobile Engineering. 206(206), 29-45.

Wong J. Y., (2009). Development of high-mobility tracked vehicles for over snow operations. Journal of Terramechanics. 46(4), 141-155.

Zongwei Y., Guoqiang W., Rui G. & Xuefei L., (2013). Theory and experimental research on six-track steering vehicles. Vehicle System Dynamics. 51(2), 218-235.

8 NOTES ON CONTRIBUTORS

Huanyu Zhao received B.E. degree from Jilin University, Changchun, China, in 2009. He is currently working towards a Ph.D. degree in the College of Mechanical Science and Engineering of Jilin University in China. His research interests include the dynamics of tracked vehicle and computer simulation.

Guoqiang Wang received Ph.D. degree in Agricultural Engineering from Jilin University of Technology (Now Jilin University), Changchun, China, in 1994. He has been a professor since 1997 in the School of Mechanical Science and Engineering, Jilin University, Changchun, China. He went to Technische Universität Bergakademie Freiberg, Germany, as a visiting scholar from 1997 to 1998 and University of Victoria, Canada, as a visiting scholar from 2003 to 2004. His research interests include modern design theories and methods (MDTM), reliability, dynamics, vibration and mechanical failure diagnosis.

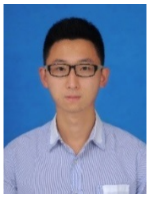

Shuai Wang received B.S. degree from Changchun University of Science and Technology, Changchun, China, in 2009. He is currently working towards a Ph.D. degree in the College of Mechanical Science and Engineering of Jilin University in China. His major area is modern mechanical design theory and method.

Ruipeng Yang received B.E. degree from Taiyuan University of Science and Technology, Taiyuan, China, in 2016. He is currently working towards a M.S. degree in the College of Mechanical Science and Engineering of Jilin University in China. His research interests include machine vision, electromechanical joint simulation and dynamic simulation.

He Tian received B.E. degree from Jilin University, Changchun, China, in 2015. He is currently working towards a M.E. degree in the College of Mechanical Science and Engineering, Jilin University in China. His research interests include the intelligent control and data acquisition.

Qiushi Bi received the M.E. degree from Jilin University, Changchun, China, in 2014. He is currently working towards a Ph.D. degree in Mechanical Engineering in the College of Mechanical Science and Engineering, Jilin University, Changchun, China. His research interests include mechanical design theory, mining machinery, DEM-FEM simulation and mechanism optimization.